

IIIb, 0.15 Å. These distortions are in line with those noted for other η^5 -indenyl complexes and show a distinct increase upon phosphine substitution.^{14b,c} Finally, it is noteworthy that the phenyl portion of the indenyl group always points away from the silyl group, even when this means it must be close to the bulky PPh₃ ligand. It seems that the silyl or methyl groups on the Fe-bonded silicon pose a greater steric impediment than the phenyl groups of the phosphine ligand. This is perhaps not surprising due to the capacity of the phenyl groups of the phosphine to take on a propeller type conformation, permitting a type of intercalation of the planar indenyl phenyl region.

A final example of the dominant steric factors in the phosphine complexes is the slight elongation of the Fe-P bonds on changing from Ib (2.207 (1) Å) to IIb (2.210 (1) Å) to IIIb (2.220 (1) Å).

In summary, the data presented in this study suggest that the role of π -bonding between the Fe and Si atoms in complexes of the type $(\eta^5\text{-C}_9\text{H}_7)\text{Fe}(\text{CO})(\text{L})\text{-silyl}$ (L = CO, PPh₃) is minimal. The "expected" shortening of the Fe-Si bond upon replacement of CO by PPh₃ is not apparent. Of the three ligands involved in the complexes upon substitution of a CO ligand by PPh₃, only the CO ligand exhibits any bond length contraction expected for increased π -bonding with the metal atom. Both the silyl and η^5 -indenyl groups exhibit bond length increases, re-

flecting the steric changes occurring. The changes in the Fe-Si bond lengths are similar for the dicarbonyl and carbonyl phosphine complexes upon changing from SiMe₃ to Si₂Me₅ to 2-Si₃Me₇. It is of course possible that any π -bonding is being overwhelmed by the increasing steric demand of the silyl and phosphine ligands at the iron atom. Further, it is possible that the Fe-Si bond lengths already are short in the $(\eta^5\text{-C}_9\text{H}_7)\text{Fe}(\text{CO})_2$ system due to π -bonding and, therefore, increases in such bonding due to the phosphine substitution are not significant. Structural analysis of complexes involving smaller phosphine ligands may provide evidence to reinforce, or counter, the first possibility, while previous spectroscopic results would seem to rule out the second.^{10,12}

Acknowledgment. This research has been supported by the Robert A. Welch Foundation, Houston, TX, and the National Science Foundation via the establishment of a Minority Research Center of Excellence in Materials Science at the University of Texas at El Paso.

Supplementary Material Available: Tables of crystal data, complete bond lengths and bond angles, anisotropic thermal parameters, and H atom parameters for Ia,b, and IIa,b, and IIIa,b (45 pages); listings of observed and calculated structure factors (85 pages). Ordering information is given on any current masthead page.

Solid-State Structure and Dynamics of a Chiral Metallacyclic (Zirconoxycarbene)tungsten Complex

Gerhard Erker,*[†] Friedrich Sosna,[†] Jeffrey L. Petersen,*[‡] Reinhard Benn,*[§] and Hildtrud Grondey[§]

*Institut für Organische Chemie der Universität Würzburg, Am Hubland, D-8700 Würzburg, FRG,
Department of Chemistry, West Virginia University, Morgantown, West Virginia 26506,
and Max-Planck-Institut für Kohlenforschung, Kaiser-Wilhelm-Platz 1, D-4330 Mülheim a.d. Ruhr, FRG*

Received December 4, 1989

The reaction of the (π -allyl)zirconoxycarbene complex $\text{Cp}_2\text{ZrOC}[\text{=W}(\text{CO})_5]\text{CH}_2\text{C}_3\text{H}_4$ (**3a**) with pinacolone affords the chiral nine-membered metallacyclic carbene complex $\text{Cp}_2\text{Zr}(\text{OC}[\text{=W}(\text{CO})_5]\text{-CH}_2\text{CH}=\text{CHCH}_2\text{CMe}(\text{CMe}_3)\text{O})$ (**5**), featuring a trans C=C double bond in the ring. In solution only one diastereoisomer is detected, being characterized by *relative* configurations of *R** and *p-S** at the chiral center and at the adjacent planar chirality element within the ring system, respectively. In contrast, the diastereomer **5'**, having *relative* configurations *R** and *p-R**, is detected as a minor component of the **3a**/pinacolone addition product in the solid state by ¹³C CP/MAS NMR spectroscopy. Complex **5** crystallizes in space group *P* $\bar{1}$ with cell parameters *a* = 8.447 (2) Å, *b* = 11.257 (3) Å, *c* = 15.224 (3) Å, α = 102.78 (2)°, β = 103.16 (2)°, γ = 99.69 (2)°, and *Z* = 2. Temperature-dependent ¹³C CP/MAS NMR spectroscopy revealed hindered rotation of the W=C(carbene) bond of **5** in the crystalline state ($\Delta G^*_{\text{rot}}(350\text{ K}) \approx 16.5\text{ kcal/mol}$).

The corresponding nine-membered metallacyclic (zirconoxycarbene)tungsten complex $\text{Cp}_2\text{Zr}(\text{OC}[\text{=W}(\text{CO})_5]\text{CH}_2\text{CH}=\text{CHCH}_2\text{CMe}_2\text{O})$ (**4**), formed by treatment of **3a** with 1 molar equiv of acetone, exhibits a W=C(carbene) rotational barrier of $\Delta G^*_{\text{rot}}(260\text{ K}) \approx 13.5\text{ kcal/mol}$ in the solid state.

Introduction

Metaloxycarbene complexes are obtained by reacting (η^2 -olefin) metallocene type reagents with metal carbonyls.¹ Typically, treatment of $\text{L}_n\text{M}(\text{CO})_m$ compounds with an equilibrium mixture of (*s-cis*-butadiene)- and (*s-trans*-butadiene)zirconocene at 25 °C affords the corresponding

(π -allyl)zirconoxycarbene complexes in good yield.² Zirconoxycarbene complexes such as $(\text{C}_5\text{H}_4\text{R})_2\text{Zr}(\text{OC}[\text{=W}(\text{CO})_5]\text{CH}_2\text{C}_3\text{H}_4)$ (**3a**, R = H; **3b**, R = CH₃) further react with ketones,³ aldehydes,^{4a} and nitriles^{4b} by means of CC

[†]Universität Würzburg.

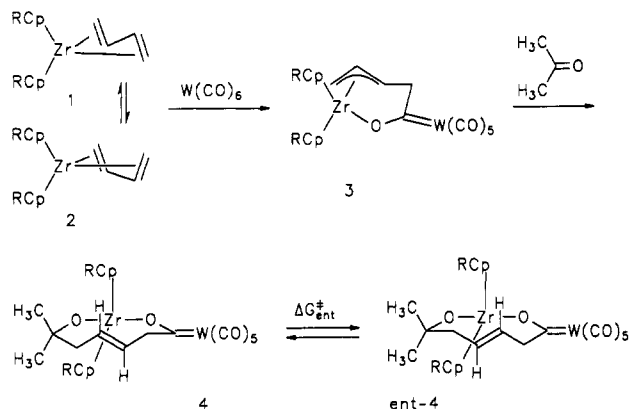
[‡]West Virginia University.

[§]Max-Planck-Institut Mülheim.

(1) Erker, G.; Dorf, U.; Benn, R.; Reinhardt, R.-D.; Petersen, J. L. *J. Am. Chem. Soc.* **1984**, *106*, 7649. Erker, G.; Dorf, U.; Mynott, R.; Tsay, Y.-H.; Krüger, C. *Angew. Chem., Int. Ed. Engl.* **1985**, *24*, 584.

(2) Review: Erker, G. *Angew. Chem.* **1989**, *101*, 411; *Angew. Chem., Int. Ed. Engl.* **1989**, *101*, 411; *Angew. Chem., Int. Ed. Engl.* **1989**, *28*, 397.

coupling of the terminal methylene carbon of the Zr-(π -allyl) moiety with the corresponding carbon of the unsaturated substrate to yield chiral nine-membered metallacyclic zirconoxycarbene complexes. For example, the reaction of **3a** with acetone produces $\text{Cp}_2\text{Zr}(\text{OC}[\text{=W}(\text{CO})_5]\text{CH}_2\text{CH}=\text{CHCH}_2\text{CMe}_2\text{O})$ (**4**), which exhibits a



trans C=C double bond in the ring. Complexes such as **4** typically feature activation barriers of enantiomerization, $\Delta G^{\ddagger}_{\text{ent}}$, of 16–17 kcal/mol as determined by dynamic ^1H NMR spectroscopic measurements.^{4b,5}

In addition to the conformational chirality element (planar chirality of the hetero *trans*-cyclononene ring⁶) of **4**, a chiral center is introduced when **3** is reacted with an aldehyde or a prochiral ketone. Thus, the reaction of **3** with pinacolone could afford two diastereomeric complexes (**5** and **5'**) that should interconvert with an activation barrier close to the one observed for the enantiomerization of **4**. However, under normal conditions of thermodynamic control, the reaction of **3a** with pinacolone proceeds with the formation of **5** in high diastereomeric excess. Herein, we describe the synthesis and characterization of **5**, which on the basis of solid-state NMR and X-ray diffraction analyses exhibits a conformational disorder of its nine-membered ring in the solid state.

Experimental Section

General Considerations. All manipulations and preparations of these organometallic compounds were performed under an argon atmosphere. For general information on the preparation and analysis of **3a**, **4**, and related metallacyclic zirconoxycarbene complexes see ref 3. ^{13}C CP/MAS NMR spectra were recorded with use of the standard CP/MAS accessory on a Bruker AM 200 spectrometer. The ^{13}C CP/MAS spectra were recorded with use of high-power proton decoupling and magic-angle spinning for line narrowing and cross polarization for sensitivity enhancement. Spinning rates were between 3000 and 4500 Hz. The 90° (^{13}C) pulse time was 5.3 μs , and the contact time was varied between 0.5 and 20 ms. In the experiments with interrupted proton decoupling⁷ for assignment of the quaternary and methyl carbon atoms the dephasing time was between 40 and 80 μs . The temperature was varied between 173 and 360 K with use of a tem-

(3) Erker, G.; Sosna, F.; Zwieter, R.; Krüger, C. *Organometallics* **1989**, *8*, 450.

(4) (a) Erker, G.; Sosna, F.; Petersen, J. L. Unpublished results. (b) See also: Erker, G.; Sosna, F.; Zwieter, R.; Krüger, C. *Z. Anorg. Allg. Chem.*, in press.

(5) Complexes of similar structural types have been obtained by reacting butadiene group 4 metallocene complexes with 2 molar equiv of the following compounds. (a) Nitrosoalkanes: Erker, G.; Humphrey, M. G. *J. Organomet. Chem.*, in press. (b) Organic carbonyl compounds: Yasuda, H.; Okamoto, T.; Matsuoka, Y.; Nakamura, A.; Kai, Y.; Kanehisa, N.; Kasai, N. *Organometallics* **1989**, *8*, 1139.

(6) See for a comparison: Cope, A. C.; Banholzer, K.; Keller, H.; Pawson, B. A.; Wang, J. J.; Winkler, H. J. S. *J. Am. Chem. Soc.* **1965**, *87*, 3644.

(7) Opella, J. S.; Frey, M. H. *J. Am. Chem. Soc.* **1979**, *101*, 5854.

Table I. Data for the X-ray Diffraction Analysis of $(\eta^5\text{-C}_5\text{H}_5)_2\text{Zr}(\text{OC}[\text{=W}(\text{CO})_5]\text{CH}_2\text{CH}=\text{CHCH}_2\text{CMe}(\text{CMe}_3)\text{O})$ (5**)**

A. Crystal Data	
cryst syst	triclinic
space group	$P\bar{1}$ (C_1^1 , No. 2)
<i>a</i> , Å	8.447 (2)
<i>b</i> , Å	11.257 (3)
<i>c</i> , Å	15.224 (3)
α , deg	102.78 (2)
β , deg	103.16 (2)
γ , deg	99.69 (2)
<i>V</i> , Å ³	1337.7 (5)
mol wt	727.58
<i>d</i> (calcd), g/cm ³	1.806
<i>Z</i>	2
μ , cm ⁻¹	49.7
B. Data Collection and Structural Analysis	
cryst dimens, mm	0.125 × 0.275 × 0.625
reflns sampled	$\pm h, \pm k, l$ ($5^\circ < 2\theta < 55^\circ$)
2θ range for centered rflns	33–35
scan rate, deg/min	2
scan width, deg	1.1 + 0.9 tan θ
no. of std rflns	3
cryst decay, %	15
total no. of measd rflns	6405
no. of unique data used	6172 ($F_o^2 > 0$)
agreement between equiv data	
$R_{\text{av}}(F_o)$	0.027
$R_{\text{av}}(F_o^2)$	0.033
transmissn coeff	0.257–0.559
<i>P</i>	0.03
discrepancy indices ($F_o^2 > \sigma(F_o^2)$)	
$R(F_o)$	0.059
$R(F_o^2)$	0.078
$R_w(F_o^2)$	0.134
σ_1	3.00
no. of variables	272
data-to-param ratio	22.7:1

perature controller and nitrogen as driving and bearing gas. Referencing of the ^{13}C shifts (± 0.1 ppm) was achieved with use of the absolute frequencies relative to the methylene carbons of adamantane ($\delta_{\text{TMS}}(\text{CH}_2) = 38.4$). Double-bearing zirconium oxide rotors of 7-mm outer diameter were filled with microcrystalline samples of **4** and **5**, respectively. For this purpose a special home-built vessel was used⁸ that permits loading of the rotor under an inert atmosphere even at low temperatures.

Reaction of **3a with Pinacolone.** To a suspension of 1.95 g (3.1 mmol) of **3a** in 60 mL of toluene was added 1 molar equiv of pinacolone (390 μL) via syringe. The mixture was stirred for 10 h at 25–30 $^\circ\text{C}$, during which time the suspension slowly dissolved. The resulting solution was decanted from a small amount of the remaining precipitate. The solution was concentrated in vacuo to about one-third of its original volume and cooled to -30°C for crystallization. The supernatant mother liquor was removed, and the remaining fine yellow crystals were dried in vacuo to give 1.58 g of **5** (70%), mp 179–180 $^\circ\text{C}$ dec. Anal. Calcd for $\text{C}_{26}\text{H}_{28}\text{O}_7\text{WZr}$ (M_r , 727.5): C, 42.92; H, 3.88. Found: C, 42.96; H, 3.87. IR: $\nu(\text{CO}) = 2057, 1964, 1911$ cm^{-1} . MS (70 eV): *m/z* 352 (5%), 324 (13), 320 (36), 296 (4), 268 (12), 240 (6), 220 (100). ^1H NMR (CDCl_3 , relative to TMS): δ 6.33, 6.26 (s, 5 H each, Cp), 5.17, 4.89 (m, 1 H each, CH=CH), 4.46, 3.16 (m, 1 H each, H5, H5'), 2.10, 1.95 (m, 1 H each, H2, H2'), 1.20 (s, 3 H, CH₃), 0.96 (s, 9 H, CMe₃); coupling constants (Hz) $^2J(\text{H},\text{H}) = 12.2$ (H2, H2'), 18.6 (H5, H5') $^3J(\text{H},\text{H}) = 11.0$ (H2, H3), 4.5 (H2', H3), 15.2 (H3, H4), 10.1 (H4, H5), 4.0 (H4, H5'). ^{13}C NMR (CDCl_3 , relative to TMS): for chemical shifts see Table IV; coupling constants (Hz) $^1J(\text{C},\text{H}) = 127$ (C2, H2, H2'), 152 (C3, H3), 152 (C4, H4), 127 (C5, H5, H5'), 125 (C(CH₃)₃), 126 (CH₃), 173 (C₅H₅); $^1J(\text{W},\text{C}) = 96.6$ (C1, W), 127.6 (cis CO, W), 123.0 (trans CO, W).

X-ray Data Collection and Structural Analysis of $\text{Cp}_2\text{Zr}(\text{OC}[\text{=W}(\text{CO})_5]\text{CH}_2\text{CH}=\text{CHCH}_2\text{CMe}(\text{CMe}_3)\text{O})$ (5**).**

(8) Grondey, H. Ph.D. Thesis, Universität Siegen, FRG, 1988. Benn, R.; Grondey, H., to be submitted for publication.

A yellow crystal of **5** was wedged into a glass capillary tube, which was sealed under a prepurified nitrogen atmosphere, and transferred and optically aligned on a Picker goniostat controlled by a Krisel Control diffractometer automation system. Procedures analogous to those described elsewhere⁹ were employed for the determination of the lattice parameters and the orientation matrix of the triclinic unit cell and for the data collection. The intensity data ($\pm h, \pm k, l$) were measured at 21 ± 1 °C with use of Zr-filtered Mo K α radiation. Duplicate reflections, which were previously corrected for sample decomposition, Lorentz-polarization, and absorption,¹⁰ were averaged, yielding 6172 unique reflections with $F_o^2 > 0$ for the structural analysis. More detailed information regarding the refined lattice parameters and the data collection procedures are summarized in Table I.

The solution and refinement of the crystal structure of **5** were complicated by the presence of a structural disorder in the crystal lattice. Initial coordinates for the tungsten atom were obtained from an analysis of the Harker vectors of an unsharpened three-dimensional Patterson map. Approximate positions of the remaining non-hydrogen atoms were located from subsequent Fourier summations. However, during the structural refinement it became immediately apparent from the unusually short C3-C4 distance of ca. 1.1 Å that the nine-membered zirconacyclic ring suffers from a structural disorder in the solid state. This problem became more evident after an anisotropic refinement of these carbon atoms, which exhibit unusually large thermal displacements normal to the ring. This disorder also extends to the methyl and *tert*-butyl groups attached to C1. Although the initial coordinates for these carbon atoms (i.e., C1 and C12-C16) provided reasonable bond angles and distances, subsequent efforts to refine these positions with anisotropic thermal parameters led to several long carbon-carbon bond distances (i.e., C1-C12 and C13-C15). Assuming that C3 and C4 are each disordered between two different sites, approximate coordinates for these sites were calculated by displacing each atom 0.35 Å in opposite directions from its averaged position along the direction of maximum thermal displacement. The corresponding pairwise C3-C4 separation between disordered sites at this point was 1.36 Å. However, all attempts to refine the coordinates of these two disordered sites failed. Their half-weighted positions always merged by returning to the original averaged position of the respective carbon atom. This difficulty is probably a consequence of the limitations of our model to incorporate other disordered features of the structure into the refinement. Although this conformational disorder prevented our efforts to determine and refine accurate positions for C3 and C4, these two atoms were included by fixing the previously estimated coordinates for their disordered sites and by varying only their isotropic temperature factor. For similar reasons, atoms C1, C12, C13, C14, C15, and C16 were varied isotropically in the final cycles of the least-squares refinement. Due to the extent of disorder of the nine-membered zirconacyclic ring of **5**, hydrogen atoms were included as fixed-atom contributions for only the cyclopentadienyl rings. Full-matrix least-squares refinement (based on F_o^2)¹¹⁻¹⁶

Table II. Positional Parameters for Non-Hydrogen Atoms in $(\eta^5\text{-C}_5\text{H}_5)_2\text{Zr}(\text{OC}[\text{=W}(\text{CO})_5]\text{CH}_2\text{CH}=\text{CHCH}_2\text{CMe}(\text{CMe}_3)\text{O})$ (5**)^a**

atom	x	y	z
W	0.04869 (4)	0.23056 (3)	0.31058 (2)
Zr	0.21835 (7)	0.67544 (5)	0.29112 (5)
O1	0.3024 (5)	0.7115 (4)	0.1900 (3)
O2	0.1786 (6)	0.4810 (4)	0.2709 (4)
O3	-0.1243 (11)	0.0455 (6)	0.4080 (6)
O4	0.1726 (11)	0.4419 (7)	0.5048 (5)
O5	-0.0620 (10)	0.0281 (7)	0.1132 (5)
O6	0.3729 (10)	0.1221 (8)	0.3542 (6)
O7	-0.2952 (9)	0.3116 (8)	0.2589 (8)
C1	0.3393 (13)	0.7088 (10)	0.1021 (8)
C2	0.4284 (12)	0.6006 (7)	0.0795 (7)
C3A	0.3232	0.5027	0.1082
C3B	0.3724	0.4697	0.0856
C4A	0.3775	0.4079	0.1380
C4B	0.3458	0.4502	0.1663
C5	0.2711 (12)	0.3269 (7)	0.1772 (7)
C6	0.1780 (8)	0.3649 (6)	0.2511 (6)
C7	-0.0656 (12)	0.1109 (8)	0.3700 (7)
C8	0.1243 (11)	0.3641 (8)	0.4343 (7)
C9	-0.1673 (12)	0.2870 (9)	0.2784 (8)
C10	-0.0239 (11)	0.1003 (9)	0.1851 (8)
C11	0.2579 (11)	0.1664 (8)	0.3402 (6)
C12	0.1665 (15)	0.6829 (11)	0.0198 (9)
C13	0.4301 (14)	0.8328 (11)	0.1025 (8)
C14	0.3409 (13)	0.9368 (10)	0.1242 (8)
C15	0.6059 (18)	0.8551 (13)	0.1870 (10)
C16	0.4700 (13)	0.8300 (10)	0.0064 (8)
C17	-0.0228 (11)	0.7439 (12)	0.3453 (7)
C18	0.0106 (14)	0.8033 (9)	0.2827 (13)
C19	-0.0327 (15)	0.7282 (20)	0.2000 (11)
C20	-0.0901 (11)	0.6130 (14)	0.2077 (10)
C21	-0.0835 (10)	0.6211 (9)	0.2991 (9)
C22	0.4720 (11)	0.8365 (8)	0.3992 (7)
C23	0.3533 (11)	0.8304 (9)	0.4466 (6)
C24	0.3261 (13)	0.7141 (10)	0.4641 (6)
C25	0.4292 (13)	0.6501 (10)	0.4302 (8)
C26	0.5221 (11)	0.7221 (11)	0.3843 (7)

^a The estimated standard deviations in parentheses for this and all subsequent tables refer to the least significant figures.

of this model converged with discrepancy indices of $R(F_o) = 0.059$, $R(F_o^2) = 0.078$, and $R_w(F_o^2) = 0.134$ with $\sigma_1 = 3.00$ for 5631 reflections with $F_o^2 > \sigma(F_o^2)$. The values of the refined positional parameters are given in Table II for all of the non-hydrogen atoms. The interatomic distances and bond angles and esd's are given in Table III. Tables of the refined thermal parameters (U_{ij} 's) and the observed and calculated structure factors are available as supplementary material.¹⁷

Results and Discussion

Spectroscopic and Structural Characterization of

5. The reaction of $\text{Cp}_2\text{Zr}(\text{OC}[\text{=W}(\text{CO})_5]\text{CH}_2\text{C}_3\text{H}_4)$ (**3a**) with 1 molar equiv of pinacolone at ambient temperature results in the formation of $\text{Cp}_2\text{Zr}(\text{OC}[\text{=W}(\text{CO})_5]\text{CH}_2\text{CH}=\text{CHCH}_2\text{CMe}(\text{CMe}_3)\text{O})$ (**5**) in 70% yield. Although this reaction could give two different diastereoisomers, NMR measurements of a solution prepared by redissolving crystals of **5** indicate that the presence of only one set of NMR signals within detection limits. The solution NMR spectra remain practically unchanged down to 173 K. At ambient temperature, the ¹H NMR spectrum of **5** in CDCl₃ is characterized by two distinct cyclopentadienyl proton resonances at δ 6.33 and 6.26. The protons of both methylene groups of the nine-membered

(9) Jones, S. B.; Petersen, J. L. *Inorg. Chem.* **1981**, *20*, 2889.

(10) The absorption correction was performed with the use of the general polyhedral shape routine of the program DTALIB. The distance from the crystal center to each face and the corresponding orientation angles (ϕ and χ) needed to place each face in diffracting position were provided to define the crystal's shape, size, and orientation with respect to the diffractometer's coordinate system.

(11) The least-squares refinement¹² of the X-ray diffraction data was based upon the minimization of $\sum w_i F_o^2 - S^2 F_c^2$, where w_i is the individual weighting factor and S is the scale factor. The discrepancy indices were calculated from the expressions $R(F_o) = \sum |F_o| - |F_c| / \sum |F_o|$, $R(F_o^2) = \sum |F_o^2 - F_c^2| / \sum F_o^2$, and $R_w(F_o^2) = [\sum w_i |F_o^2 - F_c^2|^2 / \sum w_i F_o^4]^{1/2}$. The standard deviation of an observation of unit weight, σ_1 , equals $[\sum w_i |F_o^2 - F_c^2|^2 / (n - p)]^{1/2}$, where n is the number of observations and p is the number of parameters varied during the last refinement cycle.

(12) The scattering factors employed in all of the structure factor calculations were those of Cromer and Mann¹³ for the Zr, O, and C atoms, those tabulated by Thomas and Umeda¹⁴ for W, and those of Stewart et al.¹⁵ for the hydrogen atoms. Corrections for anomalous dispersion¹⁶ were also included.

(13) Cromer, D. T.; Mann, J. B. *Acta Crystallogr., Sect. A: Cryst. Phys., Diffraction, Theor. Gen. Crystallogr.* **1968**, *A24*, 321.

(14) Thomas, L. H.; Umeda, K. *J. Chem. Phys.* **1957**, *26*, 239.

(15) Stewart, R. F.; Davidson, E. R.; Simpson, W. T. *J. Chem. Phys.* **1965**, *42*, 3175.

(16) Cromer, D. T.; Liberman, D. *J. Chem. Phys.* **1970**, *53*, 1891.

(17) The computer programs that were employed during the X-ray structural analysis are described in: Nicholson, G. A.; Petersen, J. L.; McCormick, B. *J. Inorg. Chem.* **1980**, *19*, 195.

Table III. Interatomic Distances (Å) and Bond Angles (deg) for the Non-Hydrogen Atoms in

$(\eta^5\text{-C}_5\text{H}_5)_2\text{Zr}(\text{OC}[\text{=W}(\text{CO})_5]\text{CH}_2\text{CH}=\text{CHCH}_2\text{CMe}(\text{CMe}_3)\text{O})$
(5)^{a-c}

A. Interatomic Distances			
Zr-O1	1.927 (6)	Zr-O2	2.099 (5)
Zr-C17	2.537 (12)	Zr-C22	2.520 (7)
Zr-C18	2.490 (12)	Zr-C23	2.495 (8)
Zr-C19	2.495 (17)	Zr-C24	2.494 (9)
Zr-C20	2.525 (9)	Zr-C25	2.542 (11)
Zr-C21	2.557 (9)	Zr-C26	2.536 (9)
Zr-Cp(1)	2.24 (1)	Zr-Cp(2)	2.22 (1)
W-C6	2.191 (9)	W-C9	2.023 (11)
W-C7	2.015 (11)	W-C10	2.025 (10)
W-C8	2.023 (9)	W-C11	2.015 (10)
O1-C1	1.437 (14)	O2-C6	1.274 (9)
C1-C2	1.55 (2)	C6-C5	1.54 (2)
C2-C3A	1.50	C5-C4A	1.49
C2-C3B	1.50	C5-C4B	1.49
C3A-C4A	1.36	C3B-C4B	1.36
C1-C12	1.63 (2)	C1-C13	1.47 (2)
C13-C14	1.51 (2)	C13-C15	1.67 (2)
C13-C16	1.57 (2)	C9-O7	1.150 (13)
C7-O3	1.150 (14)	C10-O5	1.148 (12)
C8-O4	1.162 (11)	C11-O6	1.163 (13)
B. Bond Angles			
O1-Zr-O2	106.6 (2)	Cp(1)-Zr-Cp(2)	126.1 (4)
Zr-O1-C1	166.0 (5)	Zr-O2-C6	168.6 (6)
O1-C1-C2	108 (1)	O2-C6-C5	113 (1)
O1-C1-C13	111 (1)	O2-C6-W	123.8 (6)
O1-C1-C12	110 (1)	W-C6-C5	123.1 (5)
C1-C2-C3A	99	C1-C2-C3B	125
C2-C3A-C4A	125	C2-C3B-C4B	120
C3A-C4A-C5	120	C3B-C4B-C5	125
C4A-C5-C6	129	C4B-C5-C6	102
C2-C1-C12	109 (1)	C1-C13-C14	114 (1)
C2-C1-C13	115 (1)	C1-C13-C15	102 (1)
C12-C1-C13	103 (1)	C1-C13-C16	111 (1)
C18-C17-C21	109 (1)	C14-C13-C15	111 (1)
C19-C18-C17	108 (1)	C14-C13-C16	108 (1)
C20-C19-C18	109 (2)	C15-C13-C16	110 (1)
C21-C20-C19	109 (1)	C7-W-C10	91.5 (4)
C17-C21-C20	106 (1)	C7-W-C11	90.4 (4)
C23-C22-C26	109 (1)	C8-W-C9	89.8 (4)
C24-C23-C22	109 (1)	C8-W-C10	178.4 (4)
C25-C24-C23	108 (1)	C8-W-C11	92.1 (4)
C26-C25-C24	110 (1)	C9-W-C10	90.2 (4)
C22-C26-C25	104 (1)	C9-W-C11	177.5 (3)
C6-W-C7	177.9 (3)	C10-W-C11	87.9 (4)
C6-W-C8	87.9 (4)	W-C7-O3	176.5 (8)
C6-W-C9	92.6 (4)	W-C8-O4	177.8 (9)
C6-W-C10	90.5 (4)	W-C9-O7	175.8 (9)
C6-W-C11	89.1 (3)	W-C10-O5	178.3 (10)
C7-W-C8	90.1 (4)	W-C11-O6	175.8 (7)
C7-W-C9	87.9 (5)		

^aThe structural parameters for C3 and C4 were calculated from unrefined disordered positions. ^bCp(n) denotes the centroid of a cyclopentadienyl ring. ^cThe esd's for the interatomic distances and bond angles were calculated from the standard errors for the fractional coordinates of the corresponding atomic positions.

ring are also diastereotopic and therefore appear as separate AB(X) multiplets with δ 2.10, 1.95 ($^2J(\text{H}, \text{H}) = 12.2$ Hz) and δ 4.46, 3.16 ($^2J(\text{H}, \text{H}) = 18.6$ Hz) for the two H atoms bound to C2 and C5, respectively. The corresponding ^1H NMR resonances of the trans CH=CH moiety appear at δ 5.17 and 4.89 with $^3J(\text{H}, \text{H}) = 15.2$ Hz. Similar proton coupling patterns have been observed for $\text{Cp}_2\text{Zr}(\text{OC}[\text{=W}(\text{CO})_5]\text{CH}_2\text{CH}=\text{CHCH}_2\text{CMe}_2\text{O})$ and related zirconoxycarbene complexes.^{3,4}

An X-ray structural analysis of **5** was undertaken to determine which of the two possible diastereomers was obtained under the reaction conditions. The molecular structure of **5** is depicted in Figure 1 with the atom-numbering scheme. The thermal ellipsoids for the non-hy-

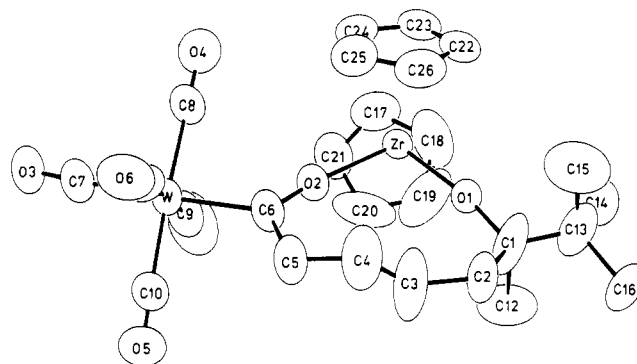


Figure 1. Perspective view of the molecular configuration of $\text{Cp}_2\text{Zr}(\text{OC}[\text{=W}(\text{CO})_5]\text{CH}_2\text{CH}=\text{CHCH}_2\text{CMe}(\text{CMe}_3)\text{O})$ with the atom-numbering scheme. The thermal ellipsoids have been scaled to enclose 50% probability. The highly anisotropic thermal motion of carbon atoms C1, C3, and C4 reflect the presence of a conformational disorder within the nine-membered zirconacyclic ring.

drogen atoms in Figure 1 are based upon a preliminary anisotropic refinement of **5** and indicate a high degree of uncertainty associated with the atomic positions for C1, C3, C4, and the substituents attached to C1. This uncertainty is probably a consequence of the presence in the crystal lattice of a conformational disorder of the trans CH=CH moiety of the metallacyclic ring. In this case, due to the inherent averaging of the X-ray diffraction method, one would expect the largest thermal displacements for these disordered atoms (within the ring) to be directed more or less perpendicular to the ring. This feature is illustrated clearly in Figure 1 for carbons C1, C3, and C4. Although an attempt to refine separate positions for the two disordered sites of C3 and C4 was unsuccessful, the size, shape, and orientation of their thermal ellipsoids are consistent with their disorder positions being displaced by ca. 0.35 Å from the respective averaged position. An analogous conformational disorder has been confronted during the X-ray structural analyses of several related compounds, including $\text{Cp}_2\text{Zr}(\text{OC}[\text{=W}(\text{CO})_5]\text{CH}_2\text{CH}=\text{CHCH}_2\text{CH}(\text{Ph})\text{O})$ ^{4a} and $(\text{C}_5\text{H}_4\text{CH}_3)_2\text{Zr}(\text{OC}[\text{=W}(\text{CO})_5]\text{CH}_2\text{CH}=\text{CHCH}_2\text{C}(\text{CMe}_3)=\text{N})$.^{4b} In the latter case, reasonable coordinates for the disordered carbon atoms of the trans CH=CH fragment were refined with use of half-weighted sites.

Despite the complications introduced by this conformational disorder, the structure determination of **5** is of sufficient quality to establish the atom connectivity and thereby allows us to assign the *relative* stereochemistry of this nine-membered zirconoxycarbene complex. Of the diastereomers described by the stereochemical notations (1-*R**)-(p-3,4,5-*S**) and (1-*R**)-(p-3,4,5-*R**) (with the non-systematic atom-numbering scheme given in Figure 1), the former is assigned to **5** according to the results of the X-ray analysis. However, in view of the inherent limitations of our structural analysis variable-temperature ^{13}C CP/MAS NMR experiments¹⁸ were undertaken to obtain further information about the solid-state disorder.

Solid-State ^{13}C NMR Studies. The ^{13}C CP/MAS NMR spectra of **5** are well-resolved with line widths averaging 25–50 Hz. The resonances of all carbon nuclei are observed, and their chemical shifts are similar to their respective values obtained from the solution ^{13}C NMR

(18) Erker, G.; Mühlenbernd, T.; Benn, R.; Rufinska, A. *Organometallics* 1986, 5, 402. Benn, R.; Grondy, H.; Nolte, R.; Erker, G. *Organometallics* 1988, 7, 777 and references cited therein.

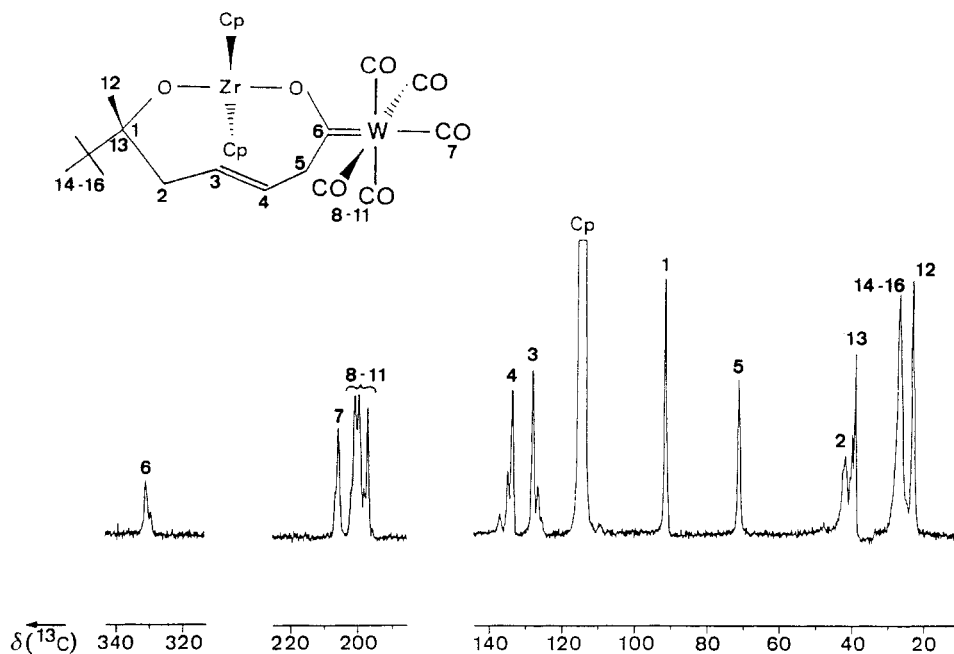


Figure 2. Solid-state ^{13}C CP/MAS NMR spectrum of a ca. 2:1 mixture of 5 and 5'.

Table IV. Comparison of Selected ^{13}C NMR Shifts of the Zirconoxycarbene Complexes 4 and 5 in Solution and in the Solid State^a

	5		4	
	soln ^b	CP/MAS ^c	soln ^b	CP/MAS ^c
C6	332.3	330.8	332.6	330.8
C5	72.2	71.3	72.1	71.6
C3/C4	133.0	133.7	132.2	133.9
	129.2	128.1	127.9	128.9
C2	41.4	41.8	48.6	49.2
C1	91.4	91.6	83.4	85.2
CH ₃	21.8	23.0	31.8	31.2
			27.9	26.8
CMe ₃	38.7	39.0		
	26.0	26.6		
CO (cis)	200.2	200.8 ^d	200.3	200.7 ^{d,e}
		199.6		199.7 ^{d,e}
		197.0		
CO (trans)	204.6	205.7	204.7	206.2 ^f
Cp	114.0	115.2	113.5	114.3
	113.3	114.0	113.1	113.8

^a Atom-numbering scheme as used for the X-ray crystal structure analysis (see Figure 1). ^b In CDCl_3 , chemical shifts referenced to tetramethylsilane, δ scale. ^c $T = 300$ K, δ scale. ^d Double intensity. ^e $T = 266$ K. ^f $^1J(\text{W}, \text{C}) = 122$ Hz (W, CO_{trans}), 128 Hz (W, CO_{cis}).

spectrum (Table IV). However, the solid-state spectra contain two similar sets of signals,¹⁹ consistent with 5 and 5' being present in an approximate ratio of 2:1. The ^{13}C

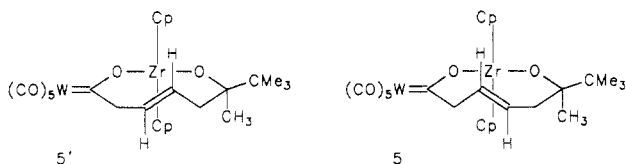


Figure 3. Deconvolution of the ^{13}C NMR resonances in the carbonyl region of the ^{13}C CP/MAS spectrum of 5.

state spectra (Figure 2) are resolved for the chiral carbon (C1), the olefinic carbons (C3 and C4), the methylene carbon (C5), and the quaternary carbon (C13) of the CMe_3 group. In addition, the line shapes of C2, C6, and the methyl carbons (C12, C14, C15, and C16) can be fitted readily to Lorentzian line profiles by assuming the presence of two isochronous chemical shifts in each case. The relative intensity of the two observed Cp signals at δ 115.2 and 114.0 (1:2) can be interpreted by assuming that 5' exhibits two unresolved C_5H_5 resonances close to the latter value. Inspection of the region containing the carbonyl resonances (see Figure 3) reveals two signals for the trans-CO group in the approximate intensity ratio of 2:1. Between δ 201 and 195 ppm three major and two minor signals for the cis-CO resonances are resolved. Detailed analysis with the line-fitting program GLINFIT shows that these signals result from four cis-CO resonances in each of the diastereomers 5 and 5', which are in the intensity ratio 2:1.

The observation of four separate resonances for the cis-CO groups of 5 (or 5') indicates that rotation about the $\text{W}=\text{C}(\text{carbene})$ bond is slow on the ^{13}C NMR time scale

NMR resonances of these two diastereomers in the solid-

(19) For a similar situation see: Erker, G.; Lecht, R.; Sosna, F.; Uhl, S.; Tsay, Y.-H.; Krüger, C.; Grondy, H.; Benn, R. *Chem. Ber.* 1988, 121, 1069.

(50 MHz) in the solid state at 300 K.²⁰ When the temperature is raised, the CP/MAS NMR spectra reveal the coalescence of these cis-CO resonances. This process is reversible. From the coalescence temperature, the activation barrier, ΔG^*_{rot} (350 K), was estimated to be 16.5 kcal/mol for this rotation in the solid state. The substituents of the nine-membered zirconacyclic ring, however, exert a significant influence on the magnitude of the $[W]=C$ rotational barrier. For the related zirconoxycarbene complex $Cp_2Zr(OC[=W(CO)_5]CH_2CH=CHCH_2CMe_2O)$ (4) only one set of ^{13}C NMR resonances are observed at 300 K in the solid state, including a single cis-CO resonance at δ 200.3 (see Table IV). This singlet separates into two lines of equal intensity at δ 201.1 and 199.7 upon lowering the monitoring temperature to 260 K. From the coalescence of the cis-CO ^{13}C resonances we have estimated a rotational activation barrier of ΔG^*_{rot} (260 K) \approx 13.5 kcal/mol for the $W=C$ bond of 4. However, at this stage a word of caution must be added. Since the frequency range within which the line shape of the CO resonances changes is very narrow and not all of the individual CO resonances are resolved, the ΔG^* values obtained for 4 and 5 can only show qualitative trends.

Concluding Remarks. The stereochemistry and dynamic behavior of these nine-membered-ring metallacyclic zirconoxycarbene complexes are remarkable in several ways. First, these complexes represent some of the very few examples^{20,21} where hindered rotation of the $L_nM=C$ linkage can be observed experimentally (albeit only in the solid state) despite the presence of an ML_n fragment (i.e., $W(CO)_5$) of high local symmetry. Moreover, it appears that the conformational equilibration of the chiral *trans*-cyclononene ring system of 4 and 5 is substantially hindered in the crystal. There is no indication from the variable-

temperature ^{13}C CP/MAS NMR spectra for the $5 \rightleftharpoons 5'$ interconversion of diastereomers taking place in the solid state. Similarly, the $4 \rightleftharpoons \text{ent-}4$ enantiomerization occurs rather rapidly in solution (ΔG^*_{ent} (323 K) = 16.6 ± 0.4 kcal/mol) but is not observed on the NMR time scale in the solid state. The solution 1H and ^{13}C NMR spectra of

$Cp_2Zr(OC[=W(CO)_5]CH_2CH=CHCH_2CMe(CMe_3)O)$ indicate that only one diastereomer (namely 5) is present under conditions where a conformational equilibration of the chiral nine-membered-ring system can occur at a sufficiently high rate.

Why is it that the same organometallic material exhibits a substantially different ratio of diastereoisomers ($5:5' \approx 2:1$) when analyzed in the solid state? We suggest that this is due to a crystallization effect. Apparently, the thermodynamically less favored diastereomer (5') preferentially crystallizes upon slowly concentrating a solution of

$Cp_2Zr(OC[=W(CO)_5]CH_2CH=CHCH_2CMe(CMe_3)O)$ in vacuo. Thereby, a noticeable amount of 5' is coprecipitated with 5. In the solid state, the $5 \rightleftharpoons 5'$ rearrangement is too slow to reestablish the equilibrium situation observed in solution. Therefore, a rather different ratio of these diastereoisomeric zirconoxycarbene complexes exists in the solid state than in solution. Furthermore, the ratio of $5:5'$ in the solid state may vary, depending on the conditions used for the crystallization of 5. It is apparent from these observations that only a combination of complementary analytical methods can give sufficient information to describe correctly even such a simple situation of equilibrating systems as the one encountered here. In some instances, a complete description of molecular structural features cannot rely solely on the results of an X-ray crystallographic analysis but may require the additional information that can be provided by solid-state CP/MAS NMR measurements.

Acknowledgment. Generous financial support from the Stiftung Volkswagenwerk, the Fonds der Chemischen Industrie, NATO (Grant No. 0346/86), and the Alfred Krupp von Bohlen und Halbach-Stiftung is gratefully acknowledged. Computer time for the X-ray structure refinement was provided by the West Virginia Network for Educational Telecomputing.

Supplementary Material Available: Listings of thermal parameters and a figure showing variable-temperature ^{13}C CP/MAS NMR spectra of 5 (3 pages); a listing of observed and calculated structure factors for 5 (22 pages). Ordering information is given on any current masthead page.

(20) This has seldom been observed for typical Fischer type carbene complexes. See e.g.: Doyle, M. J.; Lappert, M. F. *J. Chem. Soc., Chem. Commun.* **1974**, 679. Calculations: Francl, M. M.; Pietro, W. J.; Hour, R. F., Jr.; Hehre, W. J. *Organometallics* **1983**, *2*, 815. Ushio, J.; Nakatsuji, H.; Yonezawa, T. *J. Am. Chem. Soc.* **1984**, *106*, 5892. Gregory, A. R.; Mintz, E. A. *J. Am. Chem. Soc.* **1985**, *107*, 2179. Carter, E. A.; Goddard, W. A. *J. Am. Chem. Soc.* **1986**, *108*, 4746. For examples of single geometric $[M]=C(R)(O[Zr])$ isomers see: Erker, G.; Lecht, R.; Petersen, J. L.; Bönemann, H. *Organometallics* **1987**, *6*, 1962. Erker, G.; Lecht, R.; Krüger, C.; Tsay, Y.-H.; Bönemann, H. *J. Organomet. Chem.* **1987**, *326*, C75. Erker, G.; Lecht, R.; Tsay, Y.-H.; Krüger, C. *Chem. Ber.* **1987**, *120*, 1763.

(21) Dötz, K. H.; Fischer, H.; Hofmann, P.; Kreissl, F. R.; Schubert, U.; Weiss, K. *Transition Metal Carbene Complexes*; Verlag Chemie: Weinheim, FRG, 1983.